The Anthrax Protective Antigen (PA_{63}) Bound Conformation of a Peptide Inhibitor of the Binding of Lethal Factor to PA_{63}: As Determined by trNOESY NMR and Molecular Modeling†

Rickey P. Hicks,*,‡ Apurba K. Bhattacharjee,‡ Brandon W. Koser,‡ and Daniel D. Traficante§

Department of Medicinal Chemistry, Division of Experimental Therapeutics, Walter Reed Army Institute of Research, 503 Robert Grant Avenue, Silver Spring, Maryland 20910, and Naval Academy Preparatory School, Newport, Rhode Island

Received July 20, 2004

Anthrax protective antigen (PA) is one of the three proteins produced by the gram positive bacteria *Bacillus anthracis* collectively known as the "anthrax toxin" (Ascenzi, P.; Visca, P.; Ippolito, G.; Spallarossa, A.; Bolognesi, M.; et al. Anthrax toxin: a tripartite lethal combination. *FEBS Lett.* **2002**, *531*, 384−388). The role played by PA in anthrax intoxication is to transport the two enzymes lethal factor (LF) and edema factor (EF) into the cell. Collier and co-workers (Mourez, M.; Kane, R. S.; Mogridge, J.; Metallo, S.; Deschatelets, P.; et al. Designing a polyvalent inhibitor of anthrax toxin. *Nat. Biotechnol.* **2001**, 958). reported the isolation of two peptides via phage display that bind to the PA_{63} heptamer and inhibit its interaction with LF and EF, and thereby prevent the transport of LF and EF into the cell. One of these peptides, His-Thr-Ser-Thr-Try-Trp-Trp-Leu-Asp-Gly-Ala-Pro (P1), was selected for structural investigation on the basis of its ability to prevent the binding of LF to the PA_{63} heptamer bundle. Two-dimensional trNOESY experiments coupled with NOE restrained simulated annealing calculations were used to determine the PA_{63}-bound conformation of P1. On binding to PA_{63}, P1 adopts a helical conformation involving residues 3−9 while the C- and N-terminal residues exhibit dynamic fraying.

Introduction

Anthrax, from the Greek word for coal (*anthrakitis*), was the name originally given to the cutaneous illness caused by the Gram-positive bacteria *Bacillus anthracis* due to the formation of black skin lesions.[1] The name now applies to all three forms of anthrax: cutaneous, gastrointestinal, and inhalational. Most toxins that act intracellularly, such as ricin and the botulinum neurotoxins (BoNTs), are characterized as AB toxin, meaning that the toxin molecule contains two subunits, or protomers, that are released after proteolytic cleavage of the holotoxin.[1−3] Protomer A is the activating or enzymatic region, and B is the binding protomer, which interacts with a toxin-specific receptor located on the surface of the target cell.[4,5] *B. anthracis* is also characterized as an AB toxin; however, instead of one protein, the bacterium secretes three separate proteins: protective antigen (PA: 83 kDa), edema factor (EF: 89 kDa), and lethal factor (LF: 83 kDa). The combined actions of these proteins constitute the anthrax toxins which induce cell death.[5,6] It should be pointed out that each protein by itself is nontoxic.[1] The PA serves the role as the common binding protomer (protomer B), while EF and LF serve as independent A protomers, carrying out different enzymatic reactions within the host cell.[1,3]

An individual PA molecule consists of four structural domains existing mainly as antiparallel β-sheets.[1,6] Domain 1 contains binding sites for two calcium ions as well as the cleavage site for the furin protease.[1] Domain 2 is involved in pore formation and contains a large flexible loop that is believed to be involved in membrane insertion.[1] Domain 3 is involved in the formation of the heptamer bundle. Last, domain 4 binds to the anthrax toxin receptor (ATR) which is located on the surface of the host cell.[1]

The first step in anthrax intoxication is the binding of PA to the ATR. At the receptor, PA undergoes a proteolytic cleavage by furin, or a furin-like protease, at a surface loop within domain 1 to yield two fragments,[6] a 20 kDa N-terminal fragment (PA_{20}) and a 63 kDa C-terminal fragment (PA_{63}). PA_{63} remains bound to the receptor and undergoes self-assembly with other PA_{63} molecules forming a ring-shaped heptamer bundle that binds one to three molecules of EF or LF. The interaction of the seven PA_{63} molecules has been described as packing "pie wedges"[1] with the remainder of domain 1 (after proteolytic cleavage) and domain 2 lining the inside of the bundle. Domains 3 and 4 are aligned on the outside of the heptamer bundle.[1] This arrangement presents a large hydrophobic region for the binding of LF and EF.[1]

The resulting complex is transported into the cell via a receptor-mediated endocytosis, and is subsequently carried to an acidic compartment within the cell.[1] The low pH causes the PA_{63} heptamer/LF (or heptamer/EF) complex to cross the membrane into the cytosol. EF is a calcium- and CaM-dependent adenylyl cyclase that results in an increase of intracellular cAMP, which, in

* Author to whom correspondence should be addressed. Tel: (301) 319-9253. Fax: (301) 319-9449. E-mail: Rickey.Hicks@NA.AMEDD.ARMY.MIL.

† Material has been reviewed by the Walter Reed Army Institute of Research. There is no objection to its presentation and/or publications. The opinions or assertions contained herein are the private views of the author, and are not to be construed as official, or as reflecting true views of the Department of the Army or the Department of Defense.

‡ Walter Reed Army Institute of Research.

§ Naval Academy Preparatory School.

10.1021/jm040139a
Published on Web 09/18/2004

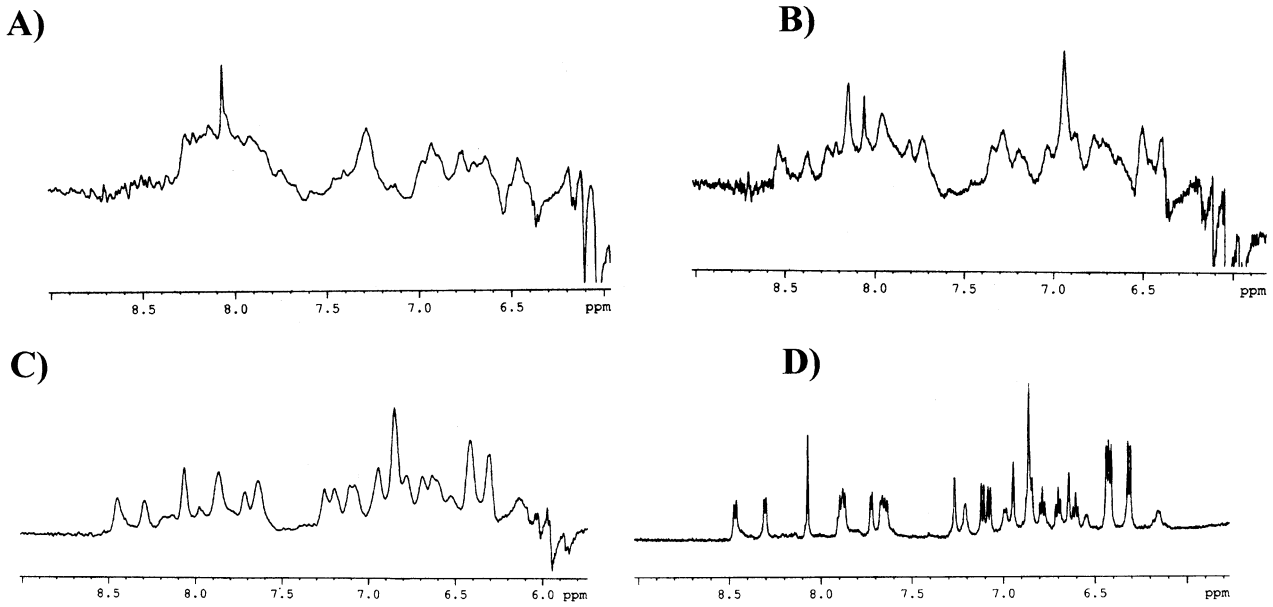

Figure 1. The ^{1}H spectra of (A) 4.76×10^{-5} M PA_{63}, (B) 4.76×10^{-5} M PA_{63} plus 5.23×10^{-4} M P1 (peptide to protein ratio 11:1) (C) 4.76×10^{-5} M PA_{63} plus 1.23×10^{-3} M P1 (peptide to protein ratio 25:1), and (D) 8.3×10^{-4} M P1 (all in 150 mM sodium acetate buffer, pH = 4.0, 277 K). As can be seen in this figure there are only minor detectable changes in chemical shift on increasing peptide concentration. A comparison of spectrum C with spectrum D shows a broadening of the resonances. This is a result of the contribution of the bound state T_2 relaxation rate as compared to the T_2 relaxation of the free state.[14,41] The observed chemical shift and line broadening behavior is consistent for the peptide in fast exchange between a bio-molecule-bound and free forms.

turn, causes disruption of intracellular communication.[7,8] EF also disrupts neutrophil function, resulting in edema. In general, death of the host is not believed to be induced by the action of EF.[7,8] LF is a metalloprotease that cleaves mitogen-activated protein (MAP) kinase-kinases, MEK1 and MEK2, at their N-terminus by hydrolyzing the Pro^8-Ile^9 amide bond of MEK1 and the Pro^{10}-Ala^{11} amide bond of MEK2.[9,10] This most likely results in the overproduction of certain lymphokines by the macrophages, and thereby causes cell death through a type of septic shock.[6]

Collier and co-workers[2] reported the isolation of two peptides via phage display that bind to the PA_{63} heptamer and inhibit its interaction with LF and EF, and thereby prevent the transport of LF and EF into the cell. The two peptides[2] consist of the following amino acid sequences: His-Thr-Ser-Thr-Tyr-Trp-Trp-Leu-Asp-Gly-Ala-Pro (P1) and His-Gln-Leu-Pro-Gln-Tyr-Tyr-Trp-Trp-Leu-Ser-Pro-Gly (P2). P1 was reported to inhibit the binding of radiolabeled LF_N (a 255-amino acid residue peptide corresponding to the N-terminal region of the PA_{63} binding domain of LF) to PA_{63} on Chinese hamster ovary (CHO) cells with an IC_{50} of approximately 150 μM.[2] Collier and Whitesides[2] developed inhibitors of the binding of LF to the PA_{63} heptameric bundle by incorporating multiple copies of P1 and P2 bound to a molecular spacer to form a polyvalent inhibitor. These polyvalent inhibitors have been shown to provide both in vivo (Fisher 344 rats, 75 nM complete protection) and in vitro (IC_{50} approximately 20 nM, CHO cells) protection against anthrax intoxication.[2] In our laboratory we are interested in determining the conformation adopted by P1 on binding to the PA_{63} heptamer bundle in aqueous solution in order to understand the structural and physicochemical requirements for binding. This information will be used to design small molecule inhibitors with improved therapeutic index compared to P1. Collier and co-workers reported that at basic and neutral pH, PA_{63} forms water soluble heptamer bundles, and at acidic pH of 5.0 or less, PA_{63} forms water soluble heptamer bundles that spontaneously insert into lipid membranes. It was therefore assumed that, under the conditions employed in this study, the majority of the PA_{63} is involved in the heptamer bundle.[11,12] No additional experiments were conducted to confirm this assumption.

Table 1. Partial Chemical Shift Assigments (ppm) for PAS1 (1.75 mg) Bound to 3.0 mg of PA_{63} (Molar Ratio 25:1 Peptide to Protein) pH = 4.0, 150 mM Sodium Acetate Buffer, Temperature = 277 K

residue	NH	αH	βH	γH	other
1 His		3.942	2.911		Ar: 0.089/6.879
2 Thr	8.454	4.004	3.798	0.792	
3 Ser	8.297	4.111	3.461/3.404		
4 Thr	7.860	3.709	3.568	0.591	
5 Tyr	7.645	3.585	2.048/1.734		Ar: 6.433/6.322
6 Trp	7.201	3.951	2.899/2.803		Ar NH: 10.083[a]
					Ar: 6.868/6.796/6.962[b]
7 Trp	6.430	3.942	2.598/1.909		Ar NH: 9.905[a]
					Ar: 6.614/6.768/6.458[b]
8 Leu	6.967	3.830	1.004	0.624	0.390
9 Asp	7.651	4.125	2.402	2.284	
10 Gly	7.890	3.486			
11 Ala	7.720	4.078	0.005		
12 Pro		3.879	1.818/1.555	1.594/1.478	3.254/3.167

[a] These assignments may be switched. [b] These assignments may be switched.

Results

The first step in this investigation was to determine whether the binding of P1 with PA_{63} occurs under the conditions of fast or slow exchange. The amide and aromatic regions of the ^{1}H spectra of (A) 4.76×10^{-5} M PA_{63}, (B) 4.76×10^{-5} M PA_{63} plus 5.23×10^{-4} M P1

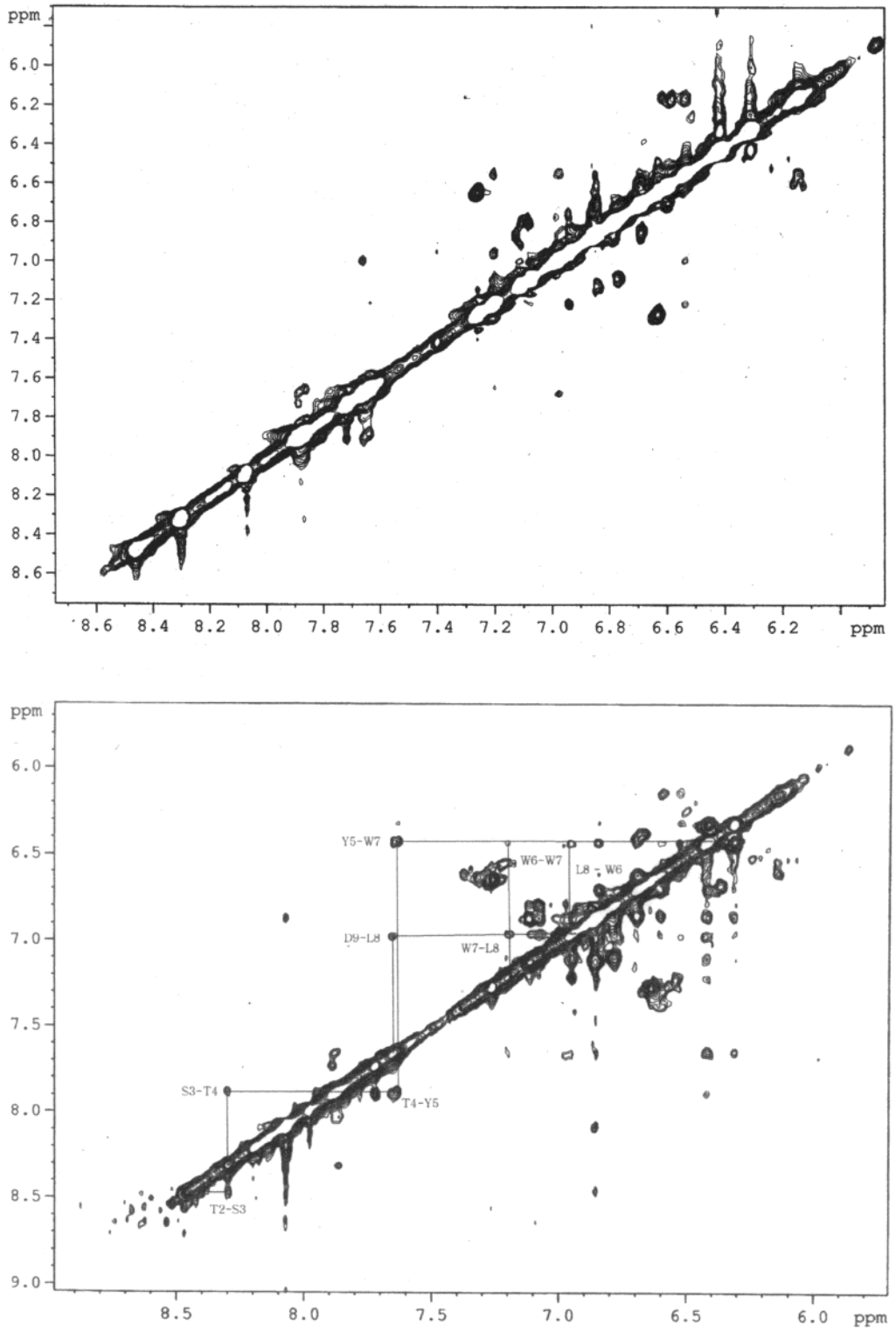

Figure 2. Top: The amide to amide region of 100 ms mixing time NOESY of P1 in buffer at 277 K. Bottom: The amide to amide region of the 100 ms mixing time trNOESY spectrum of 1.75 mg of P1 (1.23×10^{-3} M) with 3.0 mg of PA_{63} (4.76×10^{-5} M) (peptide to protein ration 25:1) in 1.0 mL (90/10 H_2O/D_2O 150 mM sodium acetate buffer, pH = 4.0). The one letter amino acid symbols are used to indicate amide proton to amide proton interactions. The spectrum was collected at a temperature of 277 K. Note that key i to $i + 1$ and i to $i + 2$ NH−NH connectivities are not observed in the trNOESY spectrum of P1 in buffer. Thus the NOEs observed in the trNOESY spectrum of P1 bound to PA_{63} must be derived from the transferred NOE effect.

(peptide to protein ratio 11:1), (C) 4.76×10^{-5} M PA_{63} plus 1.23×10^{-3} M P1, (peptide to protein ratio 25:1), and (D) 8.3×10^{-4} M P1 (all in 150 mM sodium acetate buffer, pH = 4.0, 277 K) are given in Figure 1. As can be seen in this figure, there are only minor detectable changes in chemical shift with increasing peptide concentration. A comparison of spectrum C with the spectrum of P1 in buffer (spectrum D) shows broadening of the resonance. This is due to the different T_2 relaxation rates of the peptide bound to the PA_{63} compared to the free peptide.[13] There again is no detectable change in amide chemical shifts. This obser-

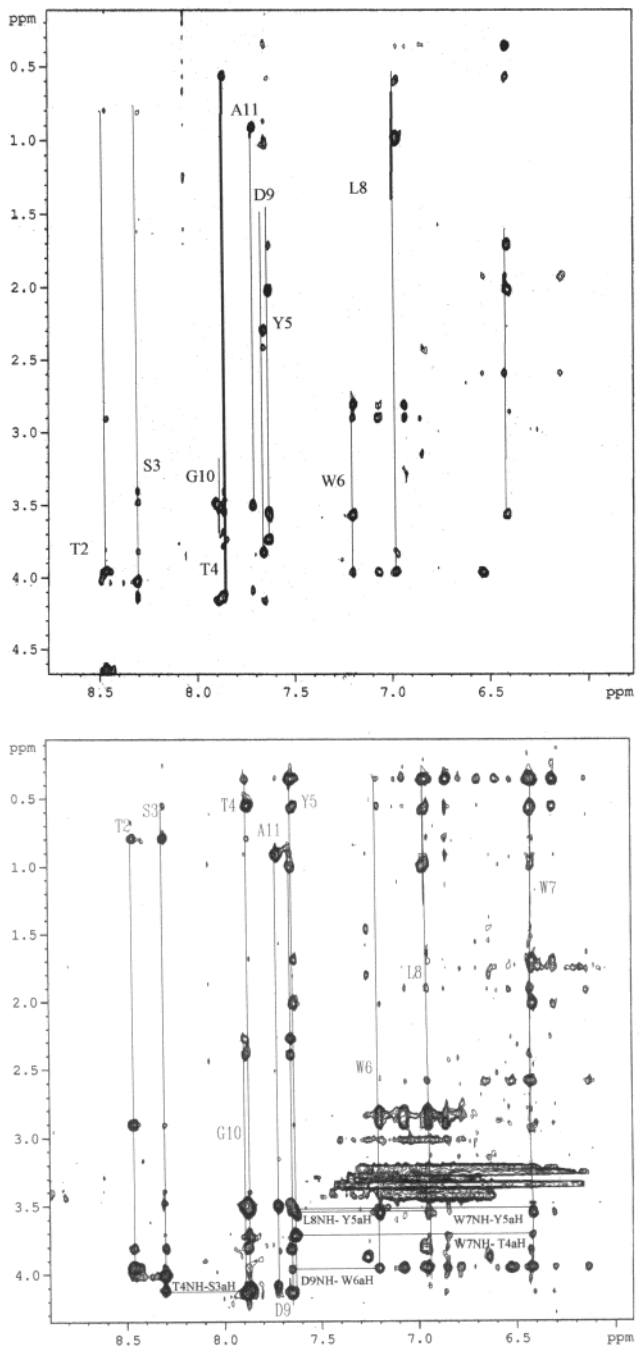

Figure 3. Top: The amide to alkyl region of 50 ms mixing time NOESY of P1 in buffer at 277 K. Bottom: The amide to amide region of the 50 ms mixing time trNOESY spectrum of 1.75 mg of P1 (1.23×10^{-3} mM) with 3.0 mg of PA_{63} (4.76×10^{-5} M) (peptide to protein ratio 25:1) in 1.0 mL (90/10 H_2O/D_2O 150 mM sodium acetate buffer, pH = 4.0). The one letter amino acid symbols are used to indicate amide proton to amide proton interactions. The spectrum was collected at a temperature of 277 K. Note that key i to $i + 1$, i to $i + 2$ and i to $i + 3$ NH−αH connectivities are not observed in the trNOESY spectrum of P1 in buffer. Thus the NOEs observed in the trNOESY spectrum of P1 bound to PA_{63} must be derived from the transferred NOE effect.

vation is consistent with "fast exchange behavior".[14] Thus, the observed NMR signals will be the weighted average of the contributions of the PA_{63}-bound and free conformers.[15] Since the concentration of the "free" peptide is approximately one and one-half orders of magnitude higher than the protein-bound peptide, the chemical shift values observed in the NMR spectrum are solely representative of the "free" conformer.[15] However, the transferred nuclear Overhauser effect is very sensitive to NOEs induced onto the free ligand by binding to the larger protein.[16−18] These NOEs are observed in the presence of "fast exchange", and they may be employed to develop information concerning the protein-bound conformation of P1.[14,19]

The second step in this investigation was to determine the protein-bound conformation of P1. Using the 2D-TOSCY[20−22] and 2D-NOESY[23] spectra, the ^1H chemical shifts for P1 (Table 1) were obtained by employing the sequence-specific resonance assignment technique developed by Wüthrich and co-workers.[24] The PA_{63}-bound conformation of P1 was determined using five trNOESY experiments. The magnetization of smaller molecules, like P1 (MW 1433), on binding to large biomolecules such as PA_{63} (MW 63000) is labeled by the magnetization of the large biomolecules. As a result, these smaller molecules yield large, negative NOEs that build up rapidly and reach a maximum intensity at relatively short mixing times. Thus, the binding of a small molecule to a large molecule can be detected by the "size, sign and build-up rates"[14] of NOEs in the trNOESY spectrum. Negative peaks were observed in the trNOESY spectra of P1 in buffer and in the presence of PA_{63}, but in the latter case the peaks were more intense. Furthermore, as illustrated in Figures 2, 3, and 4, the trNOESY spectrum of P1 bound to PA_{63} shows many more NOE cross-peaks than are observed in the trNOESY spectrum of P1 in buffer under the identical conditions. In addition, the NOE build-up rates for P1 bound to PA_{63} are very different from the NOE build-up rates of P1 in buffer. The NOE build-up rates for seven intraresidue and interresidue proton pairs of P1 bound to PA_{63} and three of these proton pairs for P1 in buffer are given in Figure 4. For P1 bound to PA_{63}, all NOE intensities reach a maximum value in the range of 50 to 100 ms, while those for P1 in buffer reach their maximum intensities in the range of 300 to 400 ms. These observations indicate that the NOEs observed for P1 bound to PA_{63} are transferred NOEs.

The following NOE connectivities in the trNOESY spectra of this P1 bound to PA_{63} are sufficient to characterize a helical secondary structure involving residues 3−9 of the peptide: (1) four sequential medium NH-NHi+1 (residues 2−6) and four sequential medium NH-NHi+1 (residues 7−11) (2) a series of sequential medium NH-NHi+2 (residues 2−4, 5−7, 6−8, 7−9, 8−10), (3) eleven sequential CαH-NHi+1, (4) four CαH-NHi+2 (residues 1−3, 4−6, 5−7, 9−11), and (5) three sequential medium CαH-NHi+3 (residues 4−7, 5−8, 6−9). These NOEs are given in Figure 6.

The NOEs observed in the trNOESY spectra of P1 bound to PA_{63} were used as restraints in NOE restrained simulated annealing calculations using a previously reported protocol to generate 100 structures of P1 bound to PA_{63}.[25] Thirty of the lowest energy structures (average energy 350.8031 kcal/mol) are shown in Figure 7 superimposing the backbone atoms of residues 3−10 onto each other. The rmsd for the superimpositions of the backbone atoms of residues 3−10 ranges from 0.206 to 1.35 Å (0.841 Å average). The average dihedral angles for these structures are given in Table

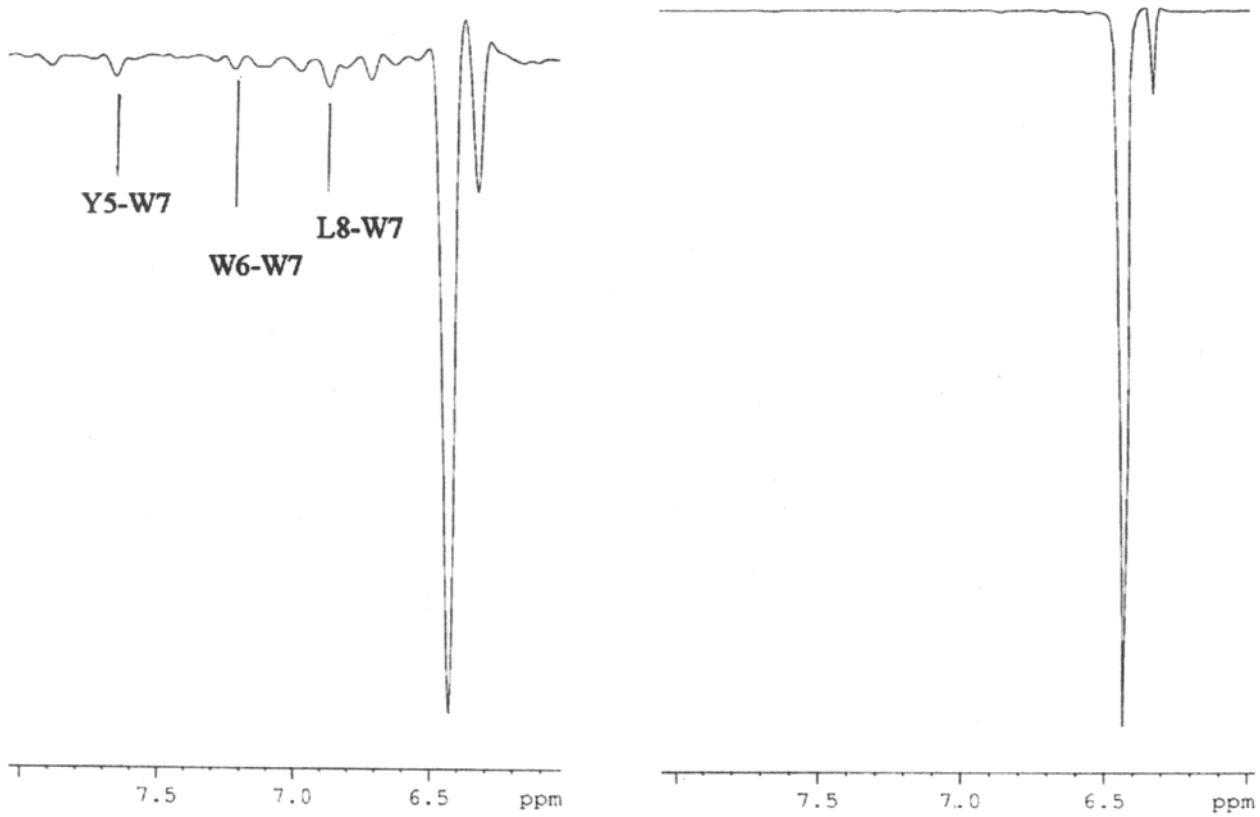

Figure 4. Scaled slices taken from the 100 ms trNOESY corresponding to the chemical shift of the Trp7 NH resonance (left) P1 bound to PA_{63} and (right) P1 in buffer only. This data clearly indicates that strong NH−NH NOEs are observed in the presence of PA_{63} only.

Table 2. Average Dihedral Angles for the 30 Low Energy Conformations for P1 Bound to the PA_{63} Heptamer Bundle

residue	av ϕ	av ψ	residue	av ϕ	av ψ
His1		57.28	Trp7	−67.29	−40.38
Thr2	−72.71	−27.03	Leu8	−73.54	−48.07
Ser3	−75.18	−29.33	Asp9	−116.07	29.60
Thr4	−79.80	−20.19	Gly10	−14.11	−11.65
Tyr5	−75.18	−39.89	Ala11	−89.30	130.99
Trp6	−70.35	−34.45	Pro12		

2. Clearly, the midregion of the peptide consisting of residues 4−8 converges to an α-helix. Residues 3 and 9, while maintaining a helical conformation, appear to be somewhat more flexible. The remaining N-terminal and C-terminal residues appear to be very flexible.

Discussion

Our NMR and NOE restrained simulated annealing calculations indicate that P1 adopts a helical structure involving residues 3−9 on binding to the PA_{63} heptamer bundle. Collier and co-workers have suggested that the tetrapeptide sequence Try^5-Trp^6-Trp^7-Leu^8 plays an important role in binding to a hydrophobic pocket near the LF binding site of PA_{63}. Our results indicate that the tetrapeptide sequence exists in the bound conformation as a very well defined α-helical structure (Figure 7). These four residues are on different faces of the helix and are not interacting with PA_{63} in a linear fashion. Therefore, it must be concluded that the relative positions of the side chains in three-dimensional space are of critical importance in binding to PA_{63}. On the basis of examination of this structure, we feel that the N-terminal His^1 residue (which is also common to P1 and P2), even though it is more conformationally flexible than residues 3−9, plays a critical role in binding by providing an electrostatic interaction on the same face of the helix as Tyr^5 and Trp^6 residues. In fact, as can be seen in Figure 8, the side chains of all three residues are very close to each other (within 7 Å). This is in contradiction to the structure proposed by Glick and co-workers.[26] This group investigated the binding interaction of the tetrapeptide Try^5-Trp^6-Trp^7-Leu^8 using conjugate gradient minimization computational methods with the crystal structure of the PA_{63} heptamer "pre-pore" reported by Petosa and co-workers.[11] Their results indicate that the tetrapeptide binds in an extended β-conformation to a hydrophobic pocket on PA_{63}-formed residues Trp^{226}, Tyr^{462}, and Phe^{464}. This discrepancy is not unexpected, since the computational methods did not involve the complete amino acid sequence of the peptide, particularly the N-terminal His^1 and the Asp^9 residues. The electrostatic potential map of the PA_{63} heptamer bundle bound conformation of P1 is shown in Figure 9. Blue regions represent positive electrostatic potential associated with the His^1 residue; the red regions represent negative electrostatic potential associated with the Asp^9 residue. The tetrapeptide sequence Tyr^5-Trp^6-Trp^7-Leu^8 connecting these two regions is electrically neutral. Since the exact binding site of P1 is still unknown, it may be reasonable to speculate from this electrostatic potential profile that the complementary binding site requires a large distribution of hydrophobic regions (white portion, Figure 9) flanked by a negative potential region (red regions) for favorable interaction with the His^1 residue and a positive poten-

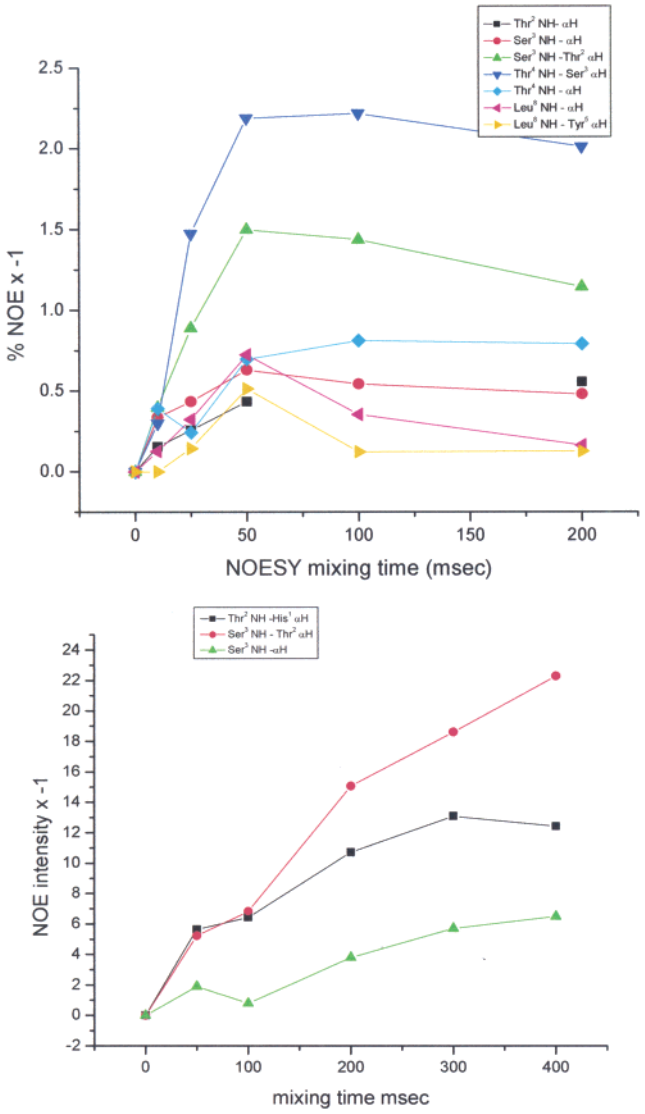

Figure 5. Top: NOE build-up rates for seven intraresidue and interresidue proton pairs of P1 bound to PA_{63}. (Dark blue triangles: $Thr^4NH-Ser^3\alpha H$. Green triangles: $Ser^3NH-Thr^2\alpha H$. Light blue tilted squares: $Thr^4NH-\alpha H$. Black squares: $Thr^2NH-\alpha H$. Red circles: $Ser^3NH-\alpha H$. Magenta triangles: $Leu^8NH-\alpha H$. Yellow triangles: $Leu^8N-Tyr^5\alpha H$.) The NOEs reach a maximum negative intensity in the mixing time range of 50 to 100 ms. This behavior is consistent with that observed with the transferred NOE effect.[14] Bottom: NOE build-up rates for three intraresidue and interresidue proton pairs of P1 in buffer only. (Red circles: $Ser^3NH-Thr^2\alpha H$. Black squares: $Thr^2NH-His^1\alpha H$. Green triangles: $Ser^3NH-\alpha H$.) The NOEs reach a maximum negative intensity in a mixing time range of 300 to 400 ms. This behavior is consistent with a "normal" NOE effect. Note that NOE intensities for the two graphs are not scaled relative to each other.

tial region (blue) for the interaction with Asp^9 residue. Thus, the electrostatic potential map clearly demonstrates that any attempt to dock only the tetrapeptide to PA_{63} will not represent the complete physicochemical surface of P1.

The overall structural requirements for binding of P1 with the PA_{63} heptamer bundle have yet to be investigated. The importance of the common hydrophobic sequence YWWL for binding to PA_{63} will be determined using selective amino acid replacement. In our opinion, the hydrophobic character of the side chains of the Tyr

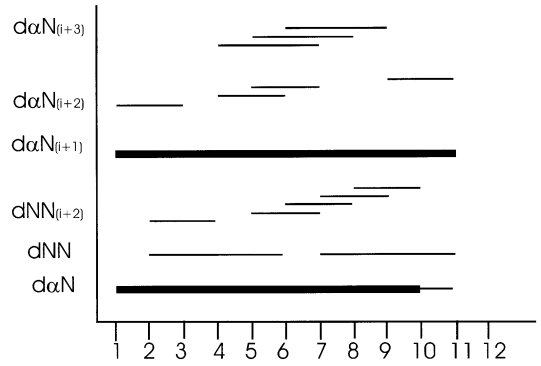

Figure 6. Key NOE connectivities used as interproton distance restraints in the simulated annealing calculations to determine the conformation of peptide 1 bound to the PA_{63}. Line thickness indicates the strength of the NOE. Strong, medium, and weak correspond to an upper distance of strong, 2.8 Å, medium 3.5 Å, and weak to very weak 4.0 and 5.0 Å.[34]

and Trp residues and the ability to act as H-bond acceptor/donator must be systematically investigated. Therefore each Tyr and Trp residue will be replaced in turn with Phe. Because the hydrophobic volume of Trp is larger than Phe, each Trp residue will also be replaced with a naphthylalanine residue (Nal). Our hypothesis concerning the importance of potential electrostatic interactions of the N-terminal His residue with the PA_{63} heptamer bundle will be tested by synthesis of two analogues of P1. The His residue will be replaced with the neutral residue Gly, and by the acidic residue Asp. Therefore to better define the structure function of P1 we proposed to synthesize the analogues given in Table 3. NMR and molecular modeling techniques will be used to determine the effect of modification on the PA_{63}-bound conformation of each analogue.

Materials and Methods

Materials. PA_{63} was purchased from List Biological Laboratories (Campbell, CA). P1 was prepared using Fmoc-based solid phase peptide synthesis by Biopeptide Company (San Diego, CA). Deuterated sodium acetate and deuterated acetic acid were purchased from Sigma Chemical Company (St. Louis, MO). Isotopically enriched ^2H_2O was purchased from Aldrich Chemical Co., Inc. (St. Louis, MO). All materials were used without further purification.

Sample Preparation. Samples were prepared for the NMR binding studies using 1.0 mL aliquots of solutions composed of 3.0 mg (4.76×10^{-5} M) of PA_{63} and 1.7 mg (1.23×10^{-3} M) of P1, in 9:1 $^1H_2O/^2H_2O$ buffered with 150 mM sodium acetate to a pH of 4.0. For the reference studies a solution of 1.7 mg (1.23×10^{-3} M) of P1 in 9:1 $^1H_2O/^2H_2O$ buffered with 150 mM sodium acetate to a pH of 4.0 was prepared.

NMR Experiments. All ^1H NMR data was collected using a Bruker Avance-600 NMR spectrometer. The application of 2D-NMR methods to investigate interactions between enzymes and substrates via the trNOESY experiment has been extensively reviewed in the literature and will not be discussed.[13,14,16−19,27−31] The proton spectrum of P1 was assigned by the interactive analysis of the 2D TOCSY[20,22] and trNOESY[14,23] spectra. The TOCSY experiment employed a modified MLEV-17[21] spin-lock sequence for a total mixing time of 80 ms, including the 2.5 ms trim pulses at the beginning and the end of the spin-lock sequence. Five trNOESY spectra of P1 bound to PA_{63} were collected with mixing times of 10, 25, 50, 100, and 200 ms. Five NOESY spectra of P1 in buffer were collected with mixing times of 50, 100, 200, 300, and 400 ms. Solvent suppression in all experiments was accomplished by application of the WATERGATE (WATER suppression by GrAdient Tailored Excitation) pulse sequence developed by

Table 3. Analogues of P1 To Be Prepared To Evaluate the Contributions of the YWWL Tetrapeptide Sequence and the His Residue to Binding Affinity to the PA_{63} Heptamer Bundle

amino acid sequence	function
His-Thr-Ser-Thr-Tyr-Trp-Trp-Leu-Asp-Gly-Ala-Pro	P1
His-Thr-Ser-Thr-Phe-Trp-Trp-Leu-Asp-Gly-Ala-Pro	H-bonding
His-Thr-Ser-Thr-Tyr-Phe-Trp-Leu-Asp-Gly-Ala-Pro	H-bonding
His-Thr-Ser-Thr-Tyr-Trp-Phe-Leu-Asp-Gly-Ala-Pro	H-bonding
His-Thr-Ser-Thr-Tyr-Trp-Trp-Phe-Asp-Gly-Ala-Pro	hydrophobic effect (Phe vs Leu)
His-Thr-Ser-Thr-Tyr-Nal-Trp-Leu-Asp-Gly-Ala-Pro	H-bonding and bulk
His-Thr-Ser-Thr-Tyr-Trp-Nal-Leu-Asp-Gly-Ala-Pro	H-bonding and bulk
Ala-Thr-Ser-Thr-Tyr-Trp-Trp-Leu-Asp-Gly-Ala-Pro	electrostatic interaction: neutral
Asp-Thr-Ser-Thr-Tyr-Trp-Trp-Leu-Asp-Gly-Ala-Pro	electrostatic interaction: negative

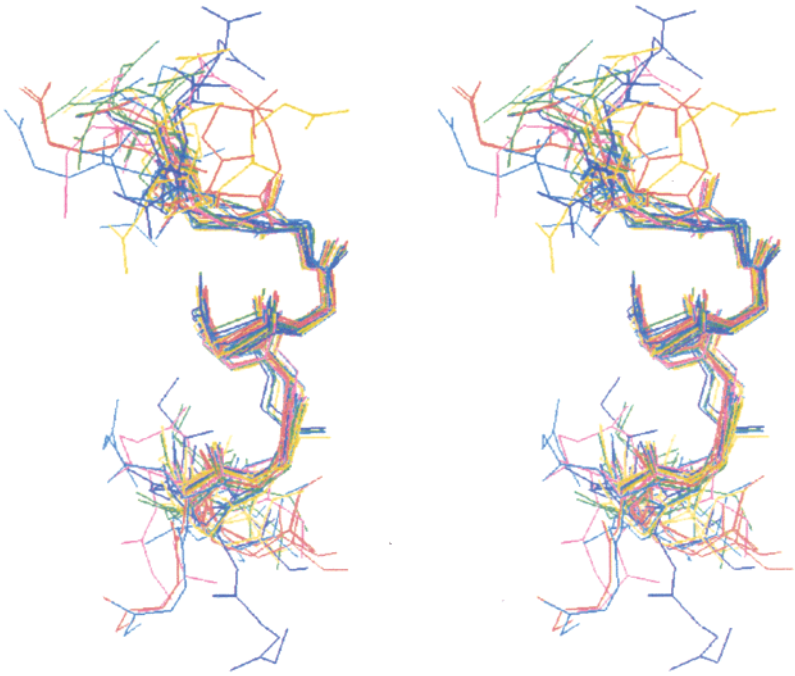

Figure 7. Stereoview of the 30 lowest energy structures (average energy 350.8031 kcal/mol) of the PA_{63}-bound conformation of P1 superimposing the backbone atoms of residues 3 to 10 onto each other. The rmsd for this superimposition ranges from 0.206 to 1.35 Å (0.841 Å, average). Clearly the midregion of the peptide consisting of residues 4−8 converges to an α-helix. Residues 3 and 9 of the helix appear to be somewhat more flexible. The remaining N-terminal and C-terminal residues appear to be very flexible.

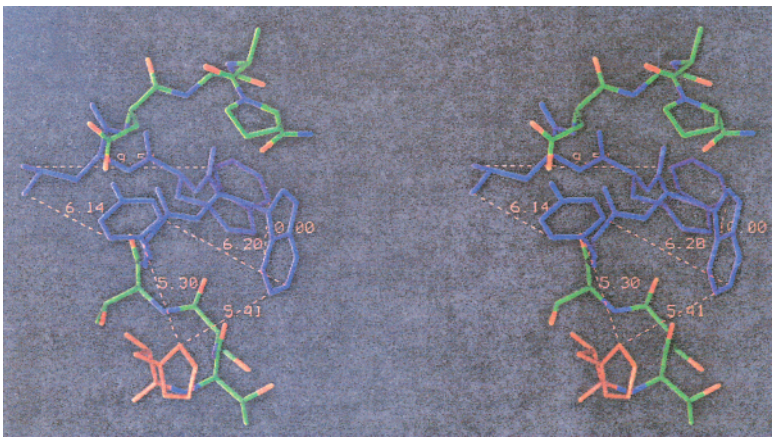

Figure 8. A stereoview of a representative structure of P1 bound to the PA_{63} heptamer bundle. Only heavy atoms are shown. The tetrapeptide Try^5-Trp^6-Trp^7-Leu^8, believed to bind with PA_{63} via hydrophobic interactions, is shown in dark blue. The N-terminal His^1 residue, which we feel plays a critical role in electrostatic interactions, is shown in red. Intramolecular distances between residues are given to highlight the closeness of particular residues to each other.

Sklenar and co-workers.[32] 2D-TOCSY spectra were collected with 64 transients and 1024 t_1 increments with a 1.5 s recycle delay for all experiments. 2D-trNOESY spectra were collected with 128 transients and 1024 t_1 increments. Data were collected at 277 K. The spectral width was 9090.9 Hz in both dimensions. All spectra were acquired with 2048 data points in F_2. All chemical shifts were referenced internally to DSS (0.00 ppm). Spectra were processed using XWINNMR (Bruker) on a Silicon Graphics O_2 workstation. Each data set was multiplied by a Gaussain window function with −10 Hz line

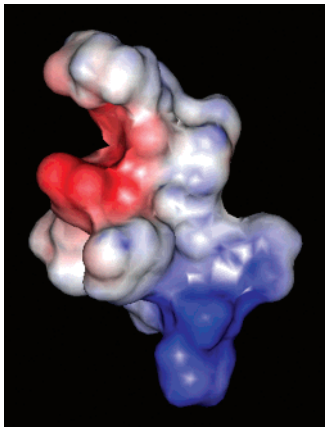

Figure 9. Electrostatic potential map of the PA_{63} heptamer bundle bound conformation of P1. Blue regions represent positive electrostatic potential associated with the His^1 residue; the red regions represent negative electrostatic potential associated with the Asp^9 residue. The tetrapeptide sequence Tyr^5-Trp^6-Trp^7-Leu^8 connecting these two regions is electrostatically neutral. This map clearly shows that any attempt to dock only the tetrapeptide to PA_{63} will not represent the physicochemical surface of P1.

broadening in each dimension before transformation to produce matrices consisting of 2048 data points in both dimensions.

Molecular Modeling. All molecular modeling experiments were performed using the Biopolymer, NMR Refine Advanced, and Discover modules of the InsightII package from Accelrys,[33] operating on a Silicon Graphics Octane workstation. Data from the five WATERGATE-trNOESY experiments were used to classify peak volumes over a range of strong to very weak, corresponding to the upper-bound interproton distance restraints of 2.8, 3.5, 4.0, and 5.0 Å [29,34−36] with strong NOEs (2.8 Å) taken from the 10 and 25 ms WATERGATE-trNOESY, medium (3.5 Å) from the 50 and 100 ms WATERGATE-trNOESY, and weak (4.0 and 5.0 Å) from the 200 ms WATERGATE-trNOESY, respectively. Since stereospecific assignments could not be made initially, pseudoatoms were employed using the center-of-mass approach, with both intraresidue and long-range correction factors added to the distance restraints.[25] In the case of terminal methyl groups, a distance correction of 0.5 Å was added to the upper limits for distance restraints.[35] After one set of MD/SA calculations, stereospecific assignments were made by manually measuring interproton distances and selecting those which were within the acceptable distance range. Correction factors were removed, and MD/SA calculations were repeated. A final set of 100 structures were generated for the PA_{63} heptamer bound P1 starting from templates with completely randomized coordinates followed by the application of a MD/SA protocol similar to that used by us earlier, for determining the SDS bound conformations of members of the tachykinin family of neuropeptides.[25,35]

Molecular Electrostatic Potentials (MEP). Molecular electrostatic potential (MEP) calculations on the peptides were performed using the DelPhi module of InsightII.[33] The algorithm allows calculation of electrostatic potential in and around a protein to be displayed as contours to gain qualitative information on protein−substrate interactions.[37−40] The generated MEP profile may be considered as an "interaction pharmacophore" of the molecule.[40]

Acknowledgment. The authors would like to acknowledge financial support from the Medical Chemical and Biological Defense Research Program of the United States Army Medical Research and Material Command.

References

(1) Ascenzi, P.; Visca, P.; Ippolito, G.; Spallarossa, A.; Bolognesi, M.; et al. Anthrax toxin: a tripartite lethal combination. *FEBS Lett.* **2002**, *531*, 384−388.
(2) Mourez, M.; Kane, R. S.; Mogridge, J.; Metallo, S.; Deschatelets, P.; et al. Designing a polyvalent inhibitor of anthrax toxin. *Nat. Biotechnol.* **2001**, 958.
(3) Humeau, Y.; Doussau, F.; Grant, N. J.; Poulain, B. How botulinum and tetanus neurotoxins block neurotransmitter release. *Biochimie* **2000**, *82*, 427−446.
(4) Swaminathan, S.; Eswaramoorthy, S. Structural analysis of the catalytic and binding sites of Clostridium botulinum neurotoxin B. *Nat. Struct. Biol.* **2000**, *7*, 693−699.
(5) Wesche, J.; Elliott, J. L.; Falnes, P. O.; Olsnes, S.; Collier, R. J. Characterization of membrane translocation by anthrax protective antigen. *Biochemistry* **1998**, *37*, 15737−15746.
(6) Stubbs, M. T. Anthrax X-rayed: new opportunities for biodefence. *TRENDS Pharmacol. Sci.* **2002**, *23*, 539−541.
(7) Dixon, T. C.; Messlson, M.; Guillemin, J.; Hanna, P. C. *N. Engl. J. Med.* **1999**, *341*, 815−826.
(8) Mourez, M.; Lacy, D. B.; Cunningham, K.; Legmann, R.; Sellman, B. R.; et al. *Trends Microbiol.* **2002**, *10*, 287−293.
(9) Vitale, G.; Pellizzari, R.; Recchi, C.; Napolitani, G.; Mock, M.; et al. Anthrax lethal factor cleaves the N-terminus of MAPKKS and induces tyrosine/threonine phosphorylation of MAPKS in cultured marcrophages. *J. Appl. Microbiol.* **1998**, *87*, 288.
(10) Duesbery, N. S.; Webb, C. P.; Leppla, S. H.; Gordon, V. M.; Klimpel, K. R.; et al. Proteolytic inactivation of MAP-kinase-kinase by anthrax lethal factor. *Science* **1998**, *280*, 734−737.
(11) Petosa, C.; Collier, R. J.; Klimpel, K. R.; Leppla, S. H.; Liddington, R. C. Crystal structure of the anthrax toxin protective antigen. *Nature* **1997**, *385*, 833−838.
(12) Milne, J. C.; Furlong, D.; Hanna, P. C.; Wall, J. S.; Collier, R. J. Anthrax protective antigen forms oligomers during intoxication of mammalian cells. *J. Biol. Chem.* **1994**, *269*, 20607−20612.
(13) Ni, F. Recent developments in transferred NOE methods. *Prog. Nucl. Magn. Reson. Spectrosc.* **1994**, *26*, 517−606.
(14) Mayer, M.; Meyer, B. Mapping the active site of angiotensin-converting enzyme by transferred NOE spectroscopy. *J. Med. Chem.* **2000**, *43*, 2093−2099.
(15) Feeney, J.; Birdsall, B. NMR studies of protein−ligand interactions. *NMR of Macromolecules. A practical Approach*; IRL Press (Oxford University Press): Oxford, 1993; pp 183−212.
(16) Craik, D. J.; Wilce, J. A. Studies of protein−ligand interactions by NMR. *Methods Mol. Biol.* **1997**, *60*, 195−232.
(17) Jarori, G. K.; Murali, N.; Nageswara Rao, B. D. Two-dimensional transferred nuclear Overhauser effect spectroscopy study of the conformation of MgATP bound at the active and ancillary sites of rabbit muscle pyruvate kinase. *Biochemistry* **1994**, *33*, 6784−6791.
(18) Murali, N.; Jarori, G. K.; Landy, S. B.; Nageswara Rao, B. D. Two-dimensional transferred nuclear Overhauser effect spectroscopy (TRNOESY) studies of nucleotide conformations in creatine kinase complexes: effects due to weak nonspecific binding. *Biochemistry* **1993**, *32*, 12941−12948.
(19) Casset, F.; Imberty, A.; Perez, S.; Etzler, M. E.; Paulsen, H.; et al. Transferred nuclear Overhauser enhancement (NOE) and rotating-frame NOE experiments reflect the size of the bound segment of the Forssman pentasaccharide in the binding site of Dolichos biflorus lectin. *Eur. J. Biochem.* **1997**, *244*, 242−250.
(20) Bax, A. Homonuclear Hartmann−Hahn experiments. *Methods Enzymol.* **1989**, *176*, 151−168.
(21) Bax, A.; Davis, D. G. MELV-17 based two-dimensional homonuclear maganetization transfer spectroscopy. *J. Magn. Reson.* **1985**, *65*, 355.
(22) Eich, G.; Bodenhausen, G.; Ernst, R. R. Coherence transfer by isotropic mixing: application to proton correlation spectroscopy. *J. Am. Chem. Soc.* **1982**, *104*, 3731.
(23) States, D. J.; Haberkon, R. A.; Rubin, D. J. A two-dimensional nuclear overhauser experiment with pure absorption phase in four quadants. *J. Magn. Reson.* **1982**, *48*, 286.
(24) Wuthrich, K.; Billeter, M.; Braun, W. Polypeptide secondary structure determination by nuclear magnetic resonance observation of short proton−proton distances. *J. Mol. Biol.* **1984**, *180*, 715−740.
(25) Young, J. K.; Hicks, R. P. NMR and molecular modeling investigations of the neuropeptide bradykinin in three different solvent systems: DMSO, 9:1 dioxane/water, and in the presence of 7.4 mM lyso phosphatidylcholine micelles. *Biopolymers* **1994**, *34*, 611−623.
(26) Glick, M.; Grant, G. H.; Richards, W. J. Pinpointing anthrax-toxin inhibitors. *Nature Biotechnol.* **2002**, *20*, 118−119.
(27) Anglister, J.; Ren, H.; Klee, C. B.; Bax, A. NMR identification of calcineurin B residues affected by binding of a calcineurin A peptide. *FEBS Lett.* **1995**, *375*, 108−112.

(28) Campbell, A. P.; Sykes, B. D. Interaction of troponium I and troponium C, use of the two-dimensional nuclear magnetic resonance transferred nuclear overhauser effect to determine the structure of the inhibitory troponium I peptide when bound to skeletal troponium C. *J. Mol. Biol.* **1991**, *222*, 405.
(29) Clore, G. M.; Gronenborn, A. M. Theory and application of the transferred nuclear overhauser effect to the study of the conformation of small ligands bound to proteins. *J. Magn. Reson.* **1982**, *48*, 402.
(30) Lippens, G.; Hallenga, K.; Belle, D. V.; Wodak, S. J.; Nirmala, N. P.; et al. Nuclear overhauser effect study of the conformation of oxytocin bound to bovine neurophysin I. *Biochemistry* **1993**, *32*, 9423.
(31) Weimar, T.; Harris, S. L.; Pitner, J. B.; Bock, K.; Pinto, B. M. Transferred nuclear Overhauser enhancement experiments show that the monoclonal antibody strep 9 selects a local minimum conformation of a *Streptococcus* group A trisaccharide−hapten. *Biochemistry* **1995**, *34*, 13672−13681.
(32) Sklenar, M.; Piotto, M.; Leppik, R.; Saudek, V. Gradient-tailored water suppression for ^{1}H-^{15}N HSQS experiments optimized to retain full sensitivity. *J. Magn. Reson., Ser. A* **1993**, *102*, 241.
(33) Accelrys, I. 9685 Scranton Road, San Diego, CA 92121-3752.
(34) Clore, G. M.; Gronenborn, A. M. Two-, three-, and four-dimensional NMR methods for obtaining larger and more precise three-dimensional structures of proteins in solution. *Annu. Rev. Biophys. Biophys. Chem.* **1991**, *20*, 29−63.
(35) Whitehead, T. L.; McNair, S. D.; Hadden, C. E.; Young, J. K.; Hicks, R. P. Membrane-induced secondary structures of neuropeptides: a comparison of the solution conformations adopted by agonists and antagonists of the mammalian tachykinin NK1 receptor. *J. Med. Chem.* **1998**, *41*, 1497−1506.
(36) Gronenborn, A. M.; Clore, G. M. Protein structure determination in solution by two-dimensional and three-dimensional nuclear magnetic resonance spectroscopy. *Anal. Chem.* **1990**, *62*, 2−15.
(37) Honig, B.; Sharp, K. A.; Yang, A.-S. Marcroscopic models of aqueous solutions: biological and chemical applications. *J. Phys. Chem.* **1993**, *97*, 1101.
(38) Gilson, M.; Honig, B. Calculation of the total electrostatic energy of a macromolecular system: solvation energies, binding energies and conformational analysis. *Protiens* **1988**, *4*, 7.
(39) Schmidt, A. B.; Fine, R. M. A CFF91-based continuum model: solvation free energies of small organic molecules and conformations of alanine dipeptide in solution. *Mol. Simul.* **1994**, *13*, 347.
(40) Nicholls, A.; Honig, B. A rapid finite difference algorithm utilizing successive over-relaxation to solve Poisson-Boltzmann equations. *J. Comput. Chem.* **1991**, *12*, 435.
(41) Behling, R. W.; Yamane, T.; Navon, G.; Sammon, M. J.; Jelinski, L. W. Measuring relative acetylcholine receptor agonist binding by selective proton nuclear magnetic resonance relaxation experiments. *Biophys. J.* **1988**, *53*, 947−954.

JM040139A